Original Article
TSL-1502, a glucuronide prodrug of a poly (ADP-ribose) polymerase (PARP) inhibitor, exhibits potent anti-tumor activity in preclinical models

Lei Wang[1,2], Xi Zhu[1,2], Lili Li[1,3], Lin Li[1,2], Li Fu[1,2], Yun Li[1,2], Haoyu Fu[1,2], Xiaoyan Chen[1,2], Liguang Lou[1,2]

[1]Shanghai Institute of Materia Medica, Chinese Academy of Sciences, 555 Zuchongzhi Road, Shanghai 201203, China; [2]University of Chinese Academy of Sciences, No. 19A Yuquan Road, Beijing 100049, China; [3]Nanjing University of Chinese Medicine, 138 Xianlin Road, Nanjing 210023, China

Abstract: Poly (ADP-ribose) polymerase (PARP) enzymes play an important role in the cellular response to DNA damage and the inhibition of PARP causes synthetic lethality in homologous recombination (HR)-deficient cancer. Multiple PARP inhibitors have been developed and have shown remarkable clinical benefits. However, treatment-related toxicities, especially the hematologic toxicities, are common and restrict the clinical applications of PARP inhibitors. In this study, we designed the first glucuronide prodrug of PARP inhibitor, TSL-1502, based on a novel and highly potent PARP inhibitor TSL-1502M. TSL-1502M exhibited promising inhibitory activity on PARP1/2, significantly induced DNA double strand breaks, G2/M arrest and apoptosis in HR-deficient cells, selectively inhibited the proliferation of HR-deficient cancer cells and sensitized both HR-deficient and HR-proficient cancer cells to conventional chemotherapy. Notably, TSL-1502M was superior to olaparib, the first-in-class PARP inhibitor, in all these processes. TSL-1502 had no inhibitory effects on PARP1/2 itself, but could selectively liberate the active drug TSL-1502M in tumor after administration in nude mice. Moreover, TSL-1502 elicited significant more potent inhibitory effects than olaparib in HR-deficient tumors, and sensitized chemotherapy in both HR-deficient and HR-proficient tumors. No severe toxicities were caused by TSL-1502 in this study. Based on the encouraging preclinical antitumor activity and the selective decomposition characteristic of TSL-1502, a clinical phase I study was initiated in China, and an Investigational New Drug (IND) was granted by the US FDA. TSL-1502 could represent a new potential therapeutic choice of PARP inhibitors.

Keywords: PARP, DNA damage, hematologic toxicity, β-glucuronidase, tumor selectivity

Introduction

Poly (ADP-ribose) polymerases (PARPs) are enzymes that catalyze the addition of polymer of ADP-ribose (PAR) adducts to their target proteins [1]. Among the PARP family members, PARP-1, -2 and -3 participate in various DNA repairing processes, with PARP-1 playing the major role [1]. Mechanically, after recognizing single strand breaks (SSBs), PARP catalyzes the synthesis of PAR by using nicotinamide adenine dinucleotide (NAD+) as a substrate, and transfers PAR to amino acid residues of various nuclear proteins [2]. PARsylation leads to the assembly of repair complex and eventually the repair of SSBs. If these processes are disturbed, SSBs will be left and finally convert to DSBs, which can normally be repaired by homologous recombination (HR). But in cells with HR defect, such as BRCA1 or BRCA2 loss, DSBs are highly lethal [3]. This synergistic cytotoxicity of PARP inhibition with mutated BRCA genes was described as synthetic lethality [4].

Based on these concepts, multiple PARP inhibitors have been studied and several clinical trials are currently exploring mono-and combination therapies in different indications [3, 5]. Among them, olaparib, rucaparib, niraparib and talazoparib have been approved by the FDA, and fluzoparib, a PARP inhibitor we previously reported [6], has been recently approved in China. PARP inhibitors have drawn increasing amount of attention due to the remarkable effi-

cacy. However, it has been reported that PARP inhibitors also impact hematopoiesis [7], which leads to severe hematologic toxicity [8]. In phase 3 trials of these inhibitors, the most common grade 3 to 4 toxicities were hematologic side effects, such as anaemia in patients treated with olaparib (19%) [9], rucaparib (19%) [10], niraparib (25%) [11] or talazoparib (39%) [12], as well as thrombocytopenia (34%) and neutropenia (20%) in patients treated with niraparib [11]. These treatment-emergent adverse events led to high frequency of dose reduction (olaparib: 25% [9], rucaparib: 55% [10], niraparib: 66% [11], talazoparib: approximately 50% [12]), and greatly restricted the clinical efficacy of PARP inhibitors. Therefore, developing PARP inhibitors with reduced toxicities, especially hematologic toxicities, is of significant clinical values.

To attenuate the adverse effects of PARP inhibitors on hematological system, one of the most promising approaches is improving drug selectivity toward tumor, such as by developing non-toxic prodrugs which could be selectively activated by enzymes in the tumor or tumor microenvironment. β-glucuronidase, a lysosomal enzyme that accumulates in the tumor microenvironment due to release from necrotic tumor cells and inflammatory cells (macrophages and neutrophils) [13, 14], can hydrolyze glucuronide prodrugs to release the active parent drug, resulting in the increased drug deposition in tumor [15]. Several glucuronide prodrugs have been studied, and displayed superior efficacy but reduced toxicity compared to standard chemotherapy [15-17]. However, no glucuronide prodrug of PARP inhibitor has been reported.

To enhance the efficacy and attenuate the serious adverse effects of existing PARP inhibitors, we extend the glucuronide pro-drugs strategy to develop PARP inhibitors. In this study, we discovered a novel, potent PARP1/2 inhibitor, TSL-1502M, which exhibited typical biochemical and cytotoxic profiles of PARP1/2 inhibitors at concentrations much lower than olaparib. We further designed a glucuronide prodrug, TSL-1502, based on TSL-1502M. TSL-1502 had no inhibitory effects on PARP1/2 itself, but could release TSL-1502M as the main product. After administration of TSL1502 in nude mice, concentrations of TSL-1502M in tumor were remarkably higher than those in plasma. Moreover, TSL-1502 elicited significant more potent inhibitory effects in HR-deficient tumors than

olaparib, and caused no severe toxicity. Because of the impressive preclinical efficacy of TSL-1502, a clinical phase I study was initiated in China, and an Investigational New Drug (IND) was granted by the US FDA. Here, we present the first report of the major preclinical pharmacological results of TSL-1502.

Material and methods

Reagents and antibodies

TSL-1502 and TSL-1502M was provided by Tasly Pharmaceutical Co., Ltd (Tianjin, China). Olaparib was from Selleckchem (Houston, TX, USA). PARP universal colorimetric assay kit and anti-PAR antibody were from Trevigen (Gaithersburg, MD, USA). Anti-RAD51 antibody was from Santa Cruz Biotechnology (Santa Cruz, CA, USA). Antibodies against γH2AX, caspase 8, caspase 3 and β-tubulin were from Cell Signaling Technology (Beverly, MA, USA). Anti-GAPDH antibody was from Protein Tech (Rosemont, IL, USA). Alexa Fluor 488-conjugated goat anti-rabbit IgG was from Molecular Probes (Eugene, OR, USA).

Cell culture

V-C8 and V-C8#13-5 cell lines were gifts from Prof. M Zdzienicka (Leiden University, Amsterdam, the Netherlands). MDA-MB-436, UWB1.289, UWB1.289+BRCA1, MX-1 and SW620 cell lines were from the American Type Culture Collection (Manassas, VA, USA). Cells were cultured according to the suppliers' instructions.

PARP1 enzyme activity

Enzyme activity was determined using PARP universal colorimetric assay kit (Trevigen Inc., Gaithersburg, MD, USA) as reported previously [18]. The incorporation of biotinylated poly (ADP-ribose) onto histone proteins was used to evaluate PARP1 enzyme activity, and the colorimetric products catalyzed by streptavidin-horseradish peroxidase was measured at 450 nm using Synergy H4 Hybrid Microplate Reader (BioTek Instruments, Winooski, VT, USA).

Molecular docking

The PARP1 structure from a crystal of PARP1/olaparib complex (PDB code: 5DS3) [19] was used as the template structure. Molecular docking was performed using Glide version 6.9

in its SP mode. LigPrep version 3.6 was applied to pre-process the compound using default parameters. The obtained docked poses were analyzed with Maestro, PyMOL and LigPlot [6].

Fluorescence microscopy

After treatment with PARP inhibitors for 24 h, cells were fixed with 4% paraformaldehyde for 15 min and permeabilized with 0.3% Triton X-100 for 10 min. Cells were then incubated with the primary antibody for 1 h and stained with Alexa Fluor 488-conjugated goat anti-rabbit IgG for 30 min. Finally, cells were counterstained with DAPI and imaged with an Olympus FV1000 confocal microscope (Tokyo, Japan).

Western blotting

After treatment with PARP inhibitors, cells were lysed in sodium dodecyl sulfate sample buffer, and Western blot analysis was conducted as described previously [20]. Proteins were separated by SDS-PAGE electrophoresis and transferred to PVDF membranes by tank blotting. After incubation with primary antibodies and secondary antibodies, proteins were visualized using the Western Blot Imaging System (Clinx Science Instruments, Shanghai, China).

Flow cytometry

Cell cycle: After treatment with PARP inhibitors for 48 h, cells were fixed in 70% ethanol, stained with propidium iodide (PI, 50 µg/ml), and subsequently analyzed by flow cytometry using a FACScan flow cytometer (BD Biosciences, San Jose, CA, USA).

Apoptosis: After treatment with PARP inhibitors for 120 h, cells were stained with Annexin V and PI using the Annexin V-FITC Apoptosis Detection Kit (Meilun Biotech, Dalian, China). Briefly, cells were resuspended in 100 µl binding buffer containing 5 µl Annexin V-FITC and 10 µl PI. After incubating for 15 min, cells were analyzed by flow cytometry.

Cell proliferation assay

Cells were treated with PARP inhibitors alone for 10 days or in combination with temozolomide/SN38 for 5 days. Sulforhodamine B assays were used to determine the effects on cells proliferation as described previously [20].

Briefly, cells were fixed with 50% trichloroacetic acid and stained with 0.04% Sulforhodamine B-acetic acid solution. Subsequently, the absorbance at 510 nm was measured using Synergy H4 Hybrid Microplate Reader (BioTek Instruments, Winooski, VT, USA).

Intracellular drug concentration

After treatment with TSL-1502 (1 µM) for 24 or 72 h, cells were rinsed with PBS and collected. Intracellular drug concentration was determined by ultra-performance liquid chromatography-ultraviolet/quadrupole-time-of-flight mass spectrometry (UPLC-UV/Q-TOF MS).

Pharmacokinetic/pharmacodynamic studies in mice

Female Balb/cA nude mice (4-5 weeks old) were purchased from Shanghai Laboratory Animal Center, Chinese Academy of Sciences (Shanghai, China). Studies were conducted by using a MDA-MB-436 xenografts model in nude mice. After a single oral (p.o.) administration of TSL-1502 (30 mg/kg), the blood and tumor tissue of mice were taken at multiple time points (0, 0.5 h, 1 h, 2 h, 4 h, 10 h, 24 h) post-dosing. Concentrations of TSL-1502 and TSL-1502M in plasma and tumor were determined by HPLC/tandem mass spectrometry. PAR formation in tumor was analyzed by Western blotting.

In vivo anti-tumor activity experiments

Tumor models were established by subcutaneously inoculating female nude mice with MDA-MB-436, MX-1 or SW620 cells. When tumors reached a volume of 100-200 mm^3, mice were randomized into control (n=12) or treatment (n=6) groups. Control group received vehicle alone, and treatment groups received administration as indicated in **Table 1**. Tumor diameter was measured by vernier calliper. Tumor volume was calculated as (length × width^2)/2, and body weight was monitored as an indicator of general health twice a week. Mice were euthanized by cervical dislocation at the end of the experiments. Tumor growth inhibition (%) was calculated as $100 - (T_t - T_0)/(C_t - C_0) \times 100$, where T_t is the mean volume of treated tumor at time t, T_0 is the mean tumor volume immediately prior to treatment (time 0), C_t is the mean tumor volume of controls at time t, and C_0 is the mean tumor volume in controls at time 0. All

Table 1. The dosage regimen of the in vivo anti-tumor activity experiments

Xenograft model	Drug	Dose (mg/kg)	Administration
MDA-MB-436	TSL-1502	5	day 0-14, BID, p.o.
		15	day 0-14, BID, p.o.
		50	day 0-14, BID, p.o.
	olaparib	50	day 0-14, BID, p.o.
MX-1	TSL-1502	25	day 0-13, BID, p.o.
		50	day 0-13, BID, p.o.
	olaparib	25	day 0-13, BID, p.o.
		50	day 0-13, BID, p.o.
	carboplatin	60	day 0, 4, 8, i.p.
	TSL-1502 + carboplatin	25; 60	day 0-13, BID, p.o.; day 0, 4, 8, i.p.
	olaparib + carboplatin	25; 60	day 0-13, BID, p.o.; day 0, 4, 8, i.p.
SW620	TSL-1502	50	day 0-16, BID, p.o.
	olaparib	30	day 0-16, BID, p.o.
	irinotecan	10	day 0, 4, i.p.
	TSL-1502 + irinotecan	5; 10	day 0-16, BID, p.o.; day 0, 4, i.p.
		15; 10	day 0-16, BID, p.o.; day 0, 4, i.p.
		50; 10	day 0-16, BID, p.o.; day 0, 4, i.p.
	olaparib+irinotecan	30; 10	day 0-16, BID, p.o.; day 0, 4, i.p.

Abbreviations: BID, twice a day; p.o., oral; i.p., intraperitoneal; day 0, the first day of administration.

animal experiments were carried out in accordance with guidelines of the Institutional Animal Care and Use Committee at the Shanghai Institute of Materia Medica, Chinese Academy of Sciences.

Statistical analysis

Data were analyzed with GraphPad Prism software. Two-tailed Student's t-tests were used to determine the statistical significance of differences between two groups.

Results

TSL-1502M is a potent inhibitor of PARP1

TSL-1502M (**Figure 1A**) displayed significantly more potent PARP1 and PARP2 inhibition effects than olaparib in a cell-free enzymatic assay (PARP1 IC_{50}: 0.66 ± 0.05 nM *versus* 6.54 ± 0.01 nM; PARP2 IC_{50}: 0.87 ± 0.17 nM *versus* 1.04 ± 0.07 nM), indicating that TSL-1502M is a potent PARP1/2 inhibitor. We then explored the binding sites of TSL-1502M in PARP1 using structural modeling. As shown in **Figure 1B**, the N and O atoms on the isoquinolin-5-one scaffold formed three hydrogen bonds with the Gly863 and Ser904 residues of PARP-1, which were also critical in the binding of PARP-1 with

olaparib and our previously reported fluzoparib [6]. To generate a non-active glucuronide prodrug, we linked a glucuronic acid to the carbonyl group in the isoquinolin-5-one scaffold, forming a new compound TSL-1502 (**Figure 1A**). Molecular docking revealed that the introduction of glucuronic acid led to spatial conflict, and TSL-1502 could not bind to Gly863 and Ser904 residues as TSL-1502M did. Instead, the O atoms on the glucuronic acid bound to Arg878 of PARP-1 (**Figure 1B**). We then tested PARP-1 inhibitory activity of TSL-1502 by enzymatic assay. Different from the highly potent inhibitory effects of TSL-1502M, the inhibitory effects of TSL-1502 on PARP1 and PARP2 were very weak (IC_{50}>3000 nM), suggesting that the inability of binding to PARP1 active sites (Gly863 and Ser904) [21] caused the loss of inhibitory activity of TSL-1502.

Release of TSL-1502M from prodrug TSL-1502

We next assessed whether the prodrug TSL-1502 could release the active parent drug TSL-1502M in cells. To this end, we treated MDA-MB-436 cells with TSL-1502 (1 μM) and determined concentrations of TSL-1502 and TSL-1502M in cells by HPLC/tandem mass spectrometry. As shown in **Figure 1C**, after treating

Figure 1. TSL-1502 is a pro-drug of PARP inhibitor TSL-1502M. A. Chemical structure of TSL-1502M and TSL-1502. B. Molecular modeling of the PARP1-TSL-1502M/TSL-1502 complex. C. MDA-MB-436 cells were treated with TSL-1502 (1 μM) for 24 or 72 h. Intracellular drug concentration was determined by UPLC-UV/Q-TOF MS.

cells for 24 and 72 h, the main product detected was TSL-1502M (24 h: 0.443 μM; 72 h: 0.281 μM), and the concentrations of TSL-1502 were very low (24 h: 0.004 μM; 72 h: 0.005

µM). These results suggest that the glucuronide-based prodrug TSL-1502 releases TSL-1502M as the main metabolite in cells.

TSL-1502 and TSL-1502M induces persistent DSBs, G2/M arrest and apoptosis in HR-deficient cells

PARP1 inhibition induces DNA SSBs, which will be then converted to DSBs during DNA replication. DSBs are highly deleterious to cells, and HR is the major pathway to repair these lesions [3]. We next investigated whether TSL-1502M showed the typical features of PARP inhibitors. Firstly, we examined the DNA damage and the subsequent effects induced by TSL-1502M in HR-proficient cells. As shown in **Figure 2A**, TSL-1502M significantly induced RAD51 foci formation, the indicator of HR repair, in V-C8#13-5 cells, indicating that HR repair process was initiated by drug-induced DSBs. Accordingly, levels of γH2AX, the marker of DSBs accumulation, in V-C8#13-5 cells did not show any significant change after drug treatment, indicating that DSBs were repaired by HR (**Figure 2B**). Then, we tested these effects in HR-deficient cells. In contrast, TSL-1502M did not induce RAD51 foci formation in V-C8 cells (BRCA2-deficient), confirming the deficiency of HR function in the cells (**Figure 2A**). As a result, the levels of γH2AX were significantly increased by TSL-1502M treatment in V-C8 cells, indicating that DSBs were left unrepaired in the cells (**Figure 2B**). These results were further supported by the induction of γH2AX levels in MDA-MB-436 cells (BRCA1-deficient) (**Figure 2B**). Collectively, these data suggest that TSL-1502M induced DNA damage, which can be repaired in HR-proficient cells, but not in HR-deficient cells, and confirm TSL-1502 as a PARP inhibitor. Notably, TSL-1502M induced a significantly more pronounced increase in γH2AX levels in HR-deficient cells compared with olaparib (about 10-fold), validating its potent inhibitory activity on PARP.

In response to DSBs, cells usually undergo G2/M phase arrest and the subsequent apoptosis [22]. TSL-1502M induced typical G2/M arrest after treatment for 48 h (**Figure 2C**), and triggered apoptosis as reflected by caspase activation (**Figure 2D**) and Annexin V binding (**Figure 2E**) after treatment for 120 h in MDA-MB-436 cells. It is noteworthy that TSL-1502M was more potent than olaparib in these processes, which was consistent with the previous results.

Together, these results suggest that TSL-1502M selectively induces persistent DSBs, G2/M arrest and apoptosis in HR-deficient cells, and displays stronger effects than olaparib.

TSL-1502 and TSL-1502M selectively inhibit the proliferation of HR-deficient cancer cells

As synthetic lethality provides a conceptual basis for the development of PARP inhibitors, we then examined whether TSL-1502M could cause synthetic lethal effects in HR-deficient cells. As shown in **Figure 3A**, TSL-1502M was preferentially efficacious against cells with HR-deficiency, such as BRCA2-deficient (V-C8) and BRCA1-deficient (MDA-MB-436 and UWB1.289) cells, and was significantly more potent than olaparib (93, 4 and 2-fold in V-C8, MDA-MB-436 and UWB1.289 cells, respectively). TSL-1502M had no obvious inhibitory effects in HR-proficient (V-C8#13-5 and UWB1.289 + BRCA1) cells. These results suggest that TSL-1502M is a potent PARP inhibitor that exhibits synthetic lethal effects in HR-deficient cells.

TSL-1502M sensitizes both HR-deficient and HR-proficient cancer cells to conventional chemotherapy

The combination of PARP inhibitor with conventional chemotherapy has been taken as a rational strategy in the clinic. We thus examined the combination effects of TSL-1502M with temozolomide (TMZ, DNA-methylating drug [23]) or SN38 (active metabolite of irinotecan, preventing religation of DNA strands [23]) in cells with different DNA repair ability. In MDA-MB-436 cells (HR-deficient), TSL-1502M potentiated the cytotoxicity of TMZ at low concentration (3 nM), and olaparib elicited similar effects at 30 nM (**Figure 3B**). In SW620 (HR-proficient) cells, TSL-1502M potentiated the cytotoxicity of SN38 at 3 µM, and these effects were similar to those produced by olaparib at 3 µM (**Figure 3C**). Collectively, the data suggest that TSL-1502M potentiates conventional chemotherapy in both HR-deficient and -proficient cells *in vitro*.

Pharmacokinetic/pharmacodynamic characteristics of TSL-1502

Given the superior activity of TSL-1502M against PARP *in vitro*, we next tested the pharmacokinetic profiles of prodrug TSL-1502 to further assess whether TSL-1502 could release TSL-1502M and elicited activity *in vivo*. After a
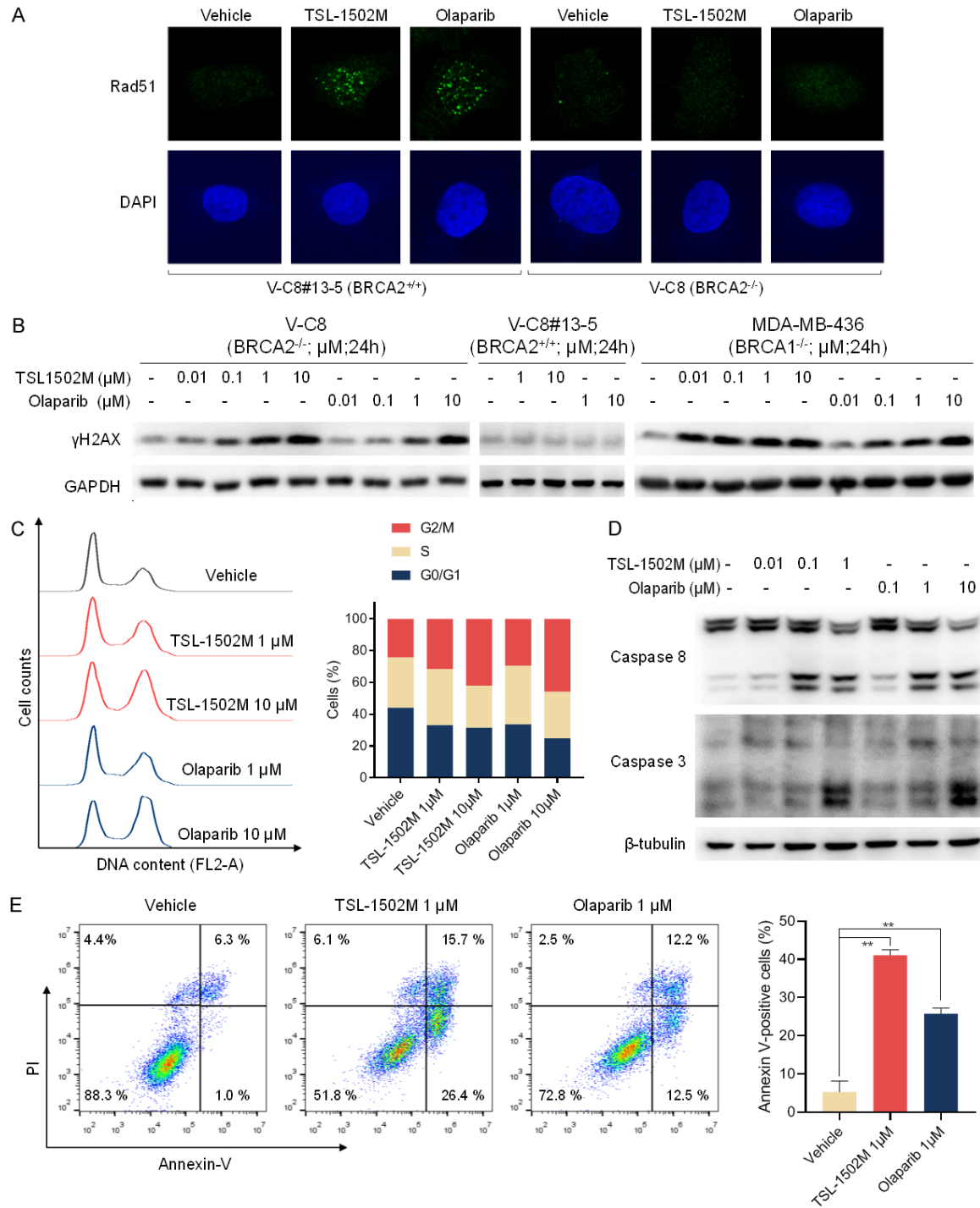
Figure 2. TSL-1502 displays typical characteristics of PARP inhibitor. A. V-C8 and V-C8#13-5 cells were treated with TSL-1502M (10 μM) or olaparib (10 μM) for 24 hours. Rad51 was detected by immunofluorescence. B. V-C8, V-C8#13-5, and MDA-MB-436 cells were treated with TSL-1502M or olaparib for 24 hours. γH2AX accumulation was assessed by western blotting. C. MDA-MB-436 cells were treated with TSL-1502M or olaparib for 48 hours. Cell cycle was analyzed by flow cytometry. D. MDA-MB-436 cells were treated with TSL-1502M or olaparib for 120 hours. The cleavage of caspase 3 and caspase 8 were detected by western blotting. E. MDA-MB-436 cells were treated with TSL-1502M or olaparib for 120 hours, stained with Annexin V and PI, and analyzed by flow cytometry. **, P < 0.01.

single oral administration of TSL-1502 at 30 mg/kg, the concentrations of TSL-1502 and

TSL-1502M were detected at different time points. As shown in **Figure 4A**, TSL-1502 was
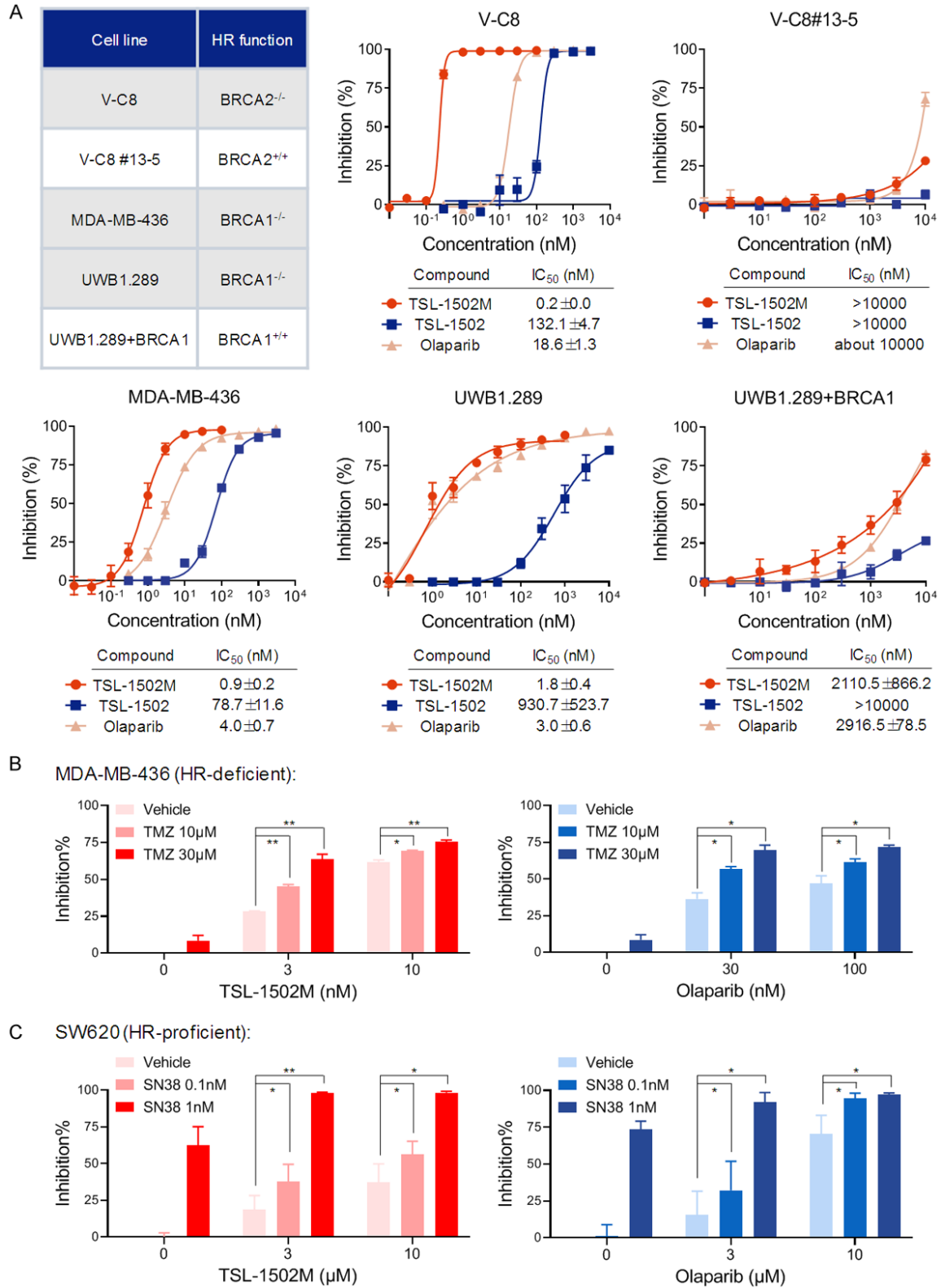
Figure 3. The inhibitory effects of TSL-1502M on cell proliferation. A. Cells were treated with different concentrations of drugs for 120 hours. B. MDA-MB-436 cells were treated with TMZ combined with TSL-1502M or olaparib for 120 hours. C. SW620 cells were treated with SN38 combined with TSL-1502M or olaparib for 120 hours. Cell proliferation was measured using sulforhodamine B assays. Data shown represent mean ± SD of 3 independent experiments. *, P < 0.05. **, P < 0.01.
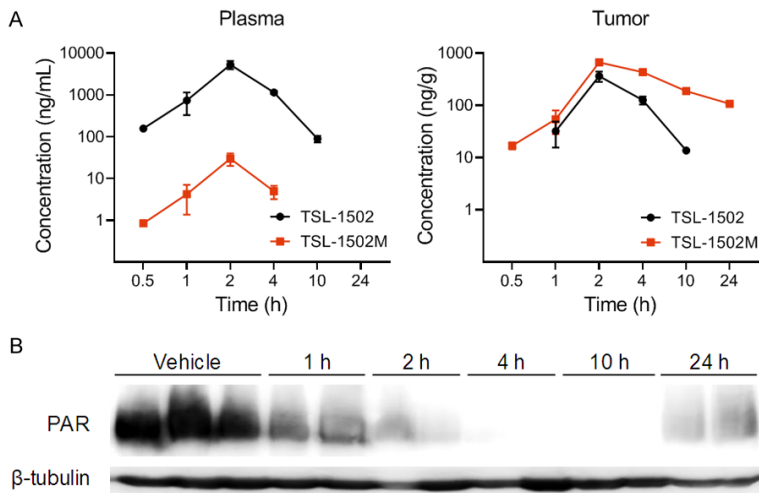
Figure 4. Pharmacokinetic/pharmacodynamic characteristics of TSL-1502. Mice bearing MDA-MB-436 xenografts were given a single oral dose of TSL-1502 (30 mg/kg). A. Concentrations of TSL-1502 and TSL-1502M in plasma and tumor were determined. B. PAR formation in tumor was analyzed by western blotting.

mainly distributed in plasma, and the C_{max} and AUC_{last} in plasma (C_{max}: 5285.0 ng/mL, AUC_{last}: 13392.2 h*ng/mL) was 14.5- and 11.9-fold higher than that in tumor (C_{max}: 363.0 ng/g, AUC_{last}: 1121.8 h*ng/g), respectively. In contrast, TSL-1502M was mainly distributed in tumor, and the C_{max} and AUC_{last} in tumor (C_{max}: 665.0 ng/g, AUC_{last}: 5397.7 h*ng/g) was 22.9- and 101.1-fold higher than that in plasma (C_{max}: 29.9 ng/mL, AUC_{last}: 53.4 h*ng/mL), respectively. The tumor concentrations of TSL-1502M were persistently higher than those of TSL-1502, and the tumor C_{max} of TSL-1502M was 2216.7-fold higher than the *in vitro* IC_{50} (0.9 nM or 0.3 ng/mL, **Figure 3A**) for inhibiting proliferation of MDA-MB-436 cells. These data suggest that TSL-1502 liberates the active component TSL-1502M mainly in tumor, resulting in a higher steady state concentration in tumor.

We further examined the effects of TSL-1502 on PAR formation, a pharmacodynamic marker reflecting the activity of PARP [24], in tumor. As shown in **Figure 4B**, TSL-1502 significantly inhibited PAR formation in a time-dependent manner in MDA-MB-436 xenografts, suggesting that TSL-1502 could inhibit the activity of PARP in tumor.

In vivo anti-tumor activity of TSL-1502 in tumor xenograft models with distinct genotypes

We first investigated the antitumor effects of TSL-1502 in MDA-MB-436 (BRCA1-deficient) xenografts models. Mice bearing MDA-MB-436 xenografts were treated with TSL-1502 at 5, 15 and 50 mg/kg (p.o., BID×15), and olaparib at 50 mg/kg (p.o., BID×15) was used as the reference. As shown in **Figure 5A**, TSL-1502 elicited dose-dependent inhibition on tumor growth, with inhibition rates of 6, 100 and 200% (day 21) at 5, 15 and 50 mg/kg, respectively. Partial tumor regression (2/6 mice, day 21) and complete tumor regression (6/6 mice, day 21) was achieved by treatment of 15 and 50 mg/kg of TSL-1502, respectively. Olaparib also inhibited tumor growth, but was less potent than TSL-1502. 50 mg/kg of olaparib led to an inhibition rate of 190% (day 21), and caused partial tumor regression in 1/6 mice and complete tumor regression in 5/6 mice (day 21). Neither TSL-1502 nor olaparib resulted in significant loss of body weight (**Figure 5A**).

We then further evaluated the antitumor effects of TSL-1502 alone and in combination with carboplatin in MX-1 (BRCA1-deficient, BRCA2-mutated) xenografts model. In the monotherapy groups, mice were treated with TSL-1502 at 25 and 50 mg/kg (p.o., BID×14), or olaparib at 25 and 50 mg/kg (p.o., BID×14). In the combination groups, mice were treated with carboplatin at 60 mg/kg (i.p., day 0, 4, 8) combined with TSL-1502 at 25 mg/kg (p.o., BID×14) or olaparib at 25 mg/kg (p.o., BID×14). As shown in **Figure 5B**, TSL-1502 inhibited the growth of tumor with inhibition rates of 71 and 91% (day 21) at 25 and 50 mg/kg, respectively. Partial tumor regression (2/6 mice, day 21) was achieved by treatment of 50 mg/kg of TSL-1502. Olaparib led to inhibition rates of 42 and 72% (day 21) at 25 and 50 mg/kg, respectively, but no tumor regression was observed. When combined with carboplatin, TSL-1502 exhibited profound anti-tumor activity with an inhibition rate of 200% (day 21) at 25 mg/kg, and led to complete tumor regression in all mice (day 37). Olaparib displayed similar antitumor effects as those of TSL-1502 when combined with carboplatin. No tumor recurrence was found in combination groups at the end of this experiment
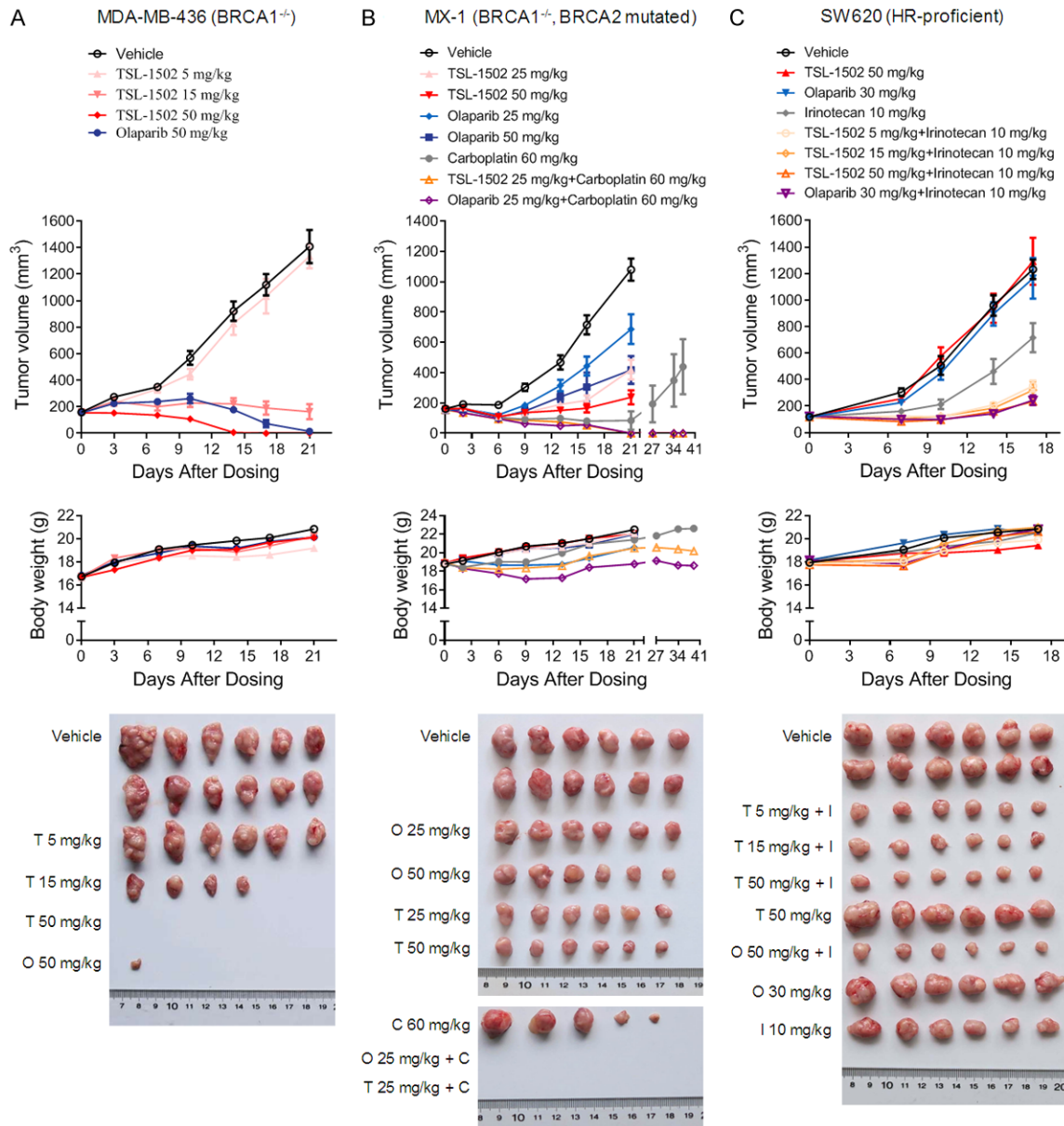
Figure 5. Antitumor activity of TSL-1502 against xenografts. Nude mice bearing MDA-MB-436 (A), MX-1 (B) and SW620 (C) xenografts were randomized into control (n = 12) or treatment (n = 6) groups, and were given treatment as indicated. Top panels, dosing schedule; bottom panels, tumor volume and body weight. Error bars represent mean ± SEM.

(day 37). Mice were generally tolerated to all these treatments. TSL-1502 combined with carboplatin caused body weight loss with a maximum of 3.8% (day 6), and olaparib combined with carboplatin caused body weight loss with a maximum of 9.3% (day 9) (**Figure 5B**). Together, TSL-1502 is more potent than olaparib alone, and both TSL-1502 and olaparib enhanced the anti-tumor activity of carboplatin in MX-1 xenografts model.

The antitumor effects of TSL-1502 alone and in combination with irinotecan in SW620 (HR-proficient) xenografts model were also investigated. As HR function of SW620 cells was proficient, SW620 xenografts model was supposed to be insensitive to PARP inhibitors. Therefore, high doses of PARP inhibitors were used in monotherapy groups: TSL1502 at 50 mg/kg (p.o., BID×17) or olaparib at 30 mg/kg (p.o., BID×17). In the combination groups, mice

were treated with irinotecan at 10 mg/kg (i.p., day 0, 4) combined with TSL-1502 at 5, 15 and 50 mg/kg (p.o., BID×17), and irinotecan combined with olaparib at intermediate dose (30 mg/kg, p.o., BID×17) was used as the reference. As shown in **Figure 5C**, TSL-1502 (50 mg/kg) alone had no apparent inhibition on tumor growth, but was extremely effective when combined with irinotecan. TSL-1502 sensitized irinotecan in a dose-dependent manner with inhibition rates of 79, 82 and 89% (day 17) at 5, 15 and 50 mg/kg, respectively. Olaparib (30 mg/kg) also enhanced the efficacy of irinotecan, leading to an inhibition rate of 89% (day 17). No enhanced toxicity was observed in either combination group (**Figure 5C**).

Collectively, TSL-1502 elicited significant more potent inhibitory effects in HR-deficient tumors than olaparib, and sensitized conventional chemotherapy in both HR-deficient and -proficient tumors. The superior *in vivo* antitumor efficacy of TSL-1502 underscores the potential use of TSL-1502 as a novel PARP inhibitor.

Discussion

PARP inhibitors have emerged as one of the most exciting new treatments for cancer. However, the clinical use of PARP inhibitors is often associated with severe hematologic side effects such as anaemia, thrombocytopenia and neutropenia [25]. In order to improve the therapeutic index and toxicity profile of PARP inhibitors, we designed the first glucuronide prodrug of PARP inhibitor, TSL-1502. A remarkable characteristic of TSL-1502 was that it exhibited superior anti-tumor activity than the classical PARP inhibitor olaparib *in vivo*, and had a favorable toxicity profile. These superiorities of TSL-1502 may come from the two below facts:

First, the active parent drug, TSL-1502M, was a highly selective and potent PARP inhibitor. TSL-1502M significantly inhibited PARP1 enzyme activity with a potency of approximately 10-fold higher than olaparib. Moreover, TSL-1502M significantly increased γH2AX levels, induced apoptosis, and caused cytotoxicity at much lower concentrations than olaparib in HR-deficient cells. TSL-1502M did not cause apparent cytotoxic effects in HR-proficient cells (similar with olaparib). Thus, TSL-1502M possessed

selective and superior antitumor activity, which may be associated with a large therapeutic window between HR-deficient and -proficient models. This superiority of TSL-1502M provided a basis for the significant anti-tumor activity and tolerable toxicity of the prodrug TSL-1502.

Second, the non-toxic prodrug TSL-1502 liberated the active component TSL-1502M mainly in tumor. TSL-1502 was a glucuronide prodrug, and had no inhibitory effects on PARP1/2 enzymatic activity itself. Therefore, TSL-1502 may have no cytotoxic effects of PARP inhibition before hydrolysis by β-glucuronidase, which presents at high levels in the tumor microenvironment [15]. As expected, TSL-1502 exhibited weak inhibitory effects on cell proliferation compared with TSL-1502M (660-fold weaker in V-C8 cells and 517-fold weaker in UWB 1.289 cells) *in vitro*, but displayed remarkable antitumor activity *in vivo*. 50 mg/kg of TSL-1502 could induce complete tumor regression (MDA-MB-436 xenografts) or partial tumor regression (MX-1 xenografts) in mice, and was more potent than olaparib. These results indicated that TSL-1502 was mainly activated *in vivo*. Indeed, TSL-1502 could release the active component TSL-1502M in MDA-MB-436 xenografts bearing mice, and primarily, in tumor. After a single oral administration of TSL-1502 at 30 mg/kg, the C_{max} and AUC_{last} of TSL-1502M in tumor was 22.9- and 101.1-fold higher than those in plasma, respectively. In contrast, the C_{max} and AUC_{last} of olaparib in tumor was about 0.37- and 0.67-fold of those in plasma, respectively, after being administered at 100 mg/kg once daily for 5 days in MDA-MB-436 xenografts bearing mice [26]. The selective activation of TSL-1502 in tumor may make it possible that TSL-1502 could be administered at relatively high doses without inducing severe toxicity.

PARP inhibitors were primarily effective against cancers in people with BRCA mutations in the clinic. To expand the indications of PARP inhibitors, great effects have been made to explore novel treatment strategies, such as combination therapies [27]. Mechanically, as PARP plays a critical role in the repair of DNA SSBs, PARP inhibitors may potentiate chemotherapy, especially DNA-damaging agents [27]. In this study, TSL-1502 significantly increased the antitumor efficacy of topoisomerase I inhibitors both *in vitro* (TSL-1502M in combination with

SN38) and *in vivo* (TSL-1502 in combination with irinotecan) in HR-proficient models. Besides, it was reported that PARP inhibitor veliparib combined with topotecan demonstrated a manageable safety profile and early signs of activity in a phase 1 clinical trial [28], and a phase 2 clinical trial is underway (NCT-01012817). These results collectively supported the further exploration of TSL-1502 in combination with irinotecan in the clinic. Moreover, PARP inhibitors also exhibited synergistic effects when combined with antiangiogenic agents. Our previous study has shown that PARP inhibitor fluzoparib in combination of apatinib, an inhibitor of vascular endothelial growth factor receptor 2, elicited significantly improved anti-tumor responses [18], and these results were further confirmed in a phase 2 clinical trial (NCT04517357). Besides, several studies reported that PARP inhibitors also enhanced immunotherapy responses [29, 30]. Interestingly, chemotherapy, antiangiogenic agents and immunotherapy could induce immune cell infiltration in tumor microenvironment, which may lead to increased secretion of β-glucuronidase [31]. Indeed, it was reported that antiangiogenic agents and immunotherapy could enhance glucuronide prodrug antitumor activity [13, 32]. As TSL-1502 is a glucuronide prodrug of PARP inhibitor, combination of TSL-1502 with chemotherapy, antiangiogenic agents and immunotherapy may have the dual advantages of PARP inhibitor and glucuronide prodrug, and further investigation is warranted.

PARP inhibitors are an exciting breakthrough in cancer treatment. However, severe hematologic side effects greatly limit the clinical use of PARP inhibitors. In this study, we developed the first glucuronide prodrug of PARP inhibitor, TSL-1502, and demonstrated that TSL-1502 could selectively liberate the active drug TSL-1502M in tumor and elicited robust *in vivo* anti-tumor efficacy without severe toxicity. Based on the encouraging preclinical results, a phase I open-label dose-escalation study is currently being conducted in patients with advanced solid tumor to evaluate the safety, tolerability, and pharmacokinetics of TSL-1502 in China, and an IND was granted a green light by the US FDA in April 2019. Taken together, our results implicate TSL-1502 as a novel promising PARP inhibitor.

Disclosure of conflict of interest

None.

Abbreviations

PARP, Poly (ADP-ribose) polymerase; HR, homologous recombination; PAR, polymer of ADP-ribose; DSB, double-strand break; SSB, single strand break; NAD+, nicotinamide adenine dinucleotide; PBS, phosphate buffered saline; PI, propidium iodide; p.o., oral; i.p., intraperitoneal; TMZ, temozolomide; BID, twice a day.

Address correspondence to: Liguang Lou, Shanghai Institute of Materia Medica, Chinese Academy of Sciences, 555 Zuchongzhi Road, Shanghai 201203, China. Tel: +86-21-50806056; Fax: +86-21-50806056; E-mail: lglou@simm.ac.cn

References

[1] McLornan DP, List A and Mufti GJ. Applying synthetic lethality for the selective targeting of cancer. N Engl J Med 2014; 371: 1725-1735.

[2] Schreiber V, Dantzer F, Ame JC and de Murcia G. Poly (ADP-ribose): novel functions for an old molecule. Nat Rev Mol Cell Biol 2006; 7: 517-528.

[3] Zheng F, Zhang Y, Chen S, Weng X, Rao Y and Fang H. Mechanism and current progress of Poly ADP-ribose polymerase (PARP) inhibitors in the treatment of ovarian cancer. Biomed Pharmacother 2020; 123: 109661.

[4] Guo GS, Zhang FM, Gao RJ, Delsite R, Feng ZH and Powell SN. DNA repair and synthetic lethality. Int J Oral Sci 2011; 3: 176-179.

[5] Gadducci A and Guerrieri ME. PARP inhibitors alone and in combination with other biological agents in homologous recombination deficient epithelial ovarian cancer: from the basic research to the clinic. Crit Rev Oncol Hematol 2017; 114: 153-165.

[6] Wang L, Yang CY, Xie CY, Jiang JH, Gao MZ, Fu L, Li Y, Bao XB, Fu HY and Lou LG. Pharmacologic characterization of fluzoparib, a novel poly (ADP-ribose) polymerase inhibitor under-

going clinical trials. Cancer Science 2019; 110: 1064-1075.

[7] Farres J, Martin-Caballero J, Martinez C, Lozano JJ, Llacuna L, Ampurdanes C, Ruiz-Herguido C, Dantzer F, Schreiber V, Villunger A, Bigas A and Yelamos J. Parp-2 is required to maintain hematopoiesis following sublethal gamma-irradiation in mice. Blood 2013; 122: 44-54.

[8] Hurvitz SA, Gonçalves A, Rugo HS, Lee KH, Fehrenbacher L, Mina LA, Diab S, Blum JL, Chakrabarti J, Elmeliegy M, DeAnnuntis L, Gauthier E, Czibere A, Tudor IC, Quek RGW, Litton JK and Ettl J. Talazoparib in patients with a germline BRCA-mutated advanced breast cancer: detailed safety analyses from the phase III EMBRACA trial. Oncologist 2019; theoncologist. 2019-0493.

[9] Pujade-Lauraine E, Ledermann JA, Selle F, Gebski V, Penson RT, Oza AM, Korach J, Huzarski T, Poveda A, Pignata S, Friedlander M, Colombo N, Harter P, Fujiwara K, Ray-Coquard I, Banerjee S, Liu J, Lowe ES, Bloomfield R and Pautier P; SOLO2/ENGOT-Ov21 investigators. Olaparib tablets as maintenance therapy in patients with platinum-sensitive, relapsed ovarian cancer and a BRCA1/2 mutation (SOLO2/ENGOT-Ov21): a double-blind, randomised, placebo-controlled, phase 3 trial. Lancet Oncol 2017; 18: 1274-1284.

[10] Coleman RL, Oza AM, Lorusso D, Aghajanian C, Oaknin A, Dean A, Colombo N, Weberpals JI, Clamp A, Scambia G, Leary A, Holloway RW, Gancedo MA, Fong PC, Goh JC, O'Malley DM, Armstrong DK, Garcia-Donas J, Swisher EM, Floquet A, Konecny GE, McNeish IA, Scott CL, Cameron T, Maloney L, Isaacson J, Goble S, Grace C, Harding TC, Raponi M, Sun J, Lin KK, Giordano H and Ledermann JA; ARIEL3 investigators. Rucaparib maintenance treatment for recurrent ovarian carcinoma after response to platinum therapy (ARIEL3): a randomised, double-blind, placebo-controlled, phase 3 trial. Lancet 2017; 390: 1949-1961.

[11] Mirza MR, Monk BJ, Herrstedt J, Oza AM, Mahner S, Redondo A, Fabbro M, Ledermann JA, Lorusso D, Vergote I, Ben-Baruch NE, Marth C, Madry R, Christensen RD, Berek JS, Dorum A, Tinker AV, du Bois A, Gonzalez-Martin A, Follana P, Benigno B, Rosenberg P, Gilbert L, Rimel BJ, Buscema J, Balser JP, Agarwal S and Matulonis UA; ENGOT-OV16/NOVA Investigators. Niraparib maintenance therapy in platinum-sensitive, recurrent ovarian cancer. N Engl J Med 2016; 375: 2154-2164.

[12] Litton JK, Rugo HS, Ettl J, Hurvitz SA, Goncalves A, Lee KH, Fehrenbacher L, Yerushalmi R, Mina LA, Martin M, Roche H, Im YH, Quek RGW, Markova D, Tudor IC, Hannah AL, Eiermann W and Blum JL. Talazoparib in patients with advanced breast cancer and a germline BRCA mutation. N Engl J Med 2018; 379: 753-763.

[13] Juan TY, Roffler SR, Hou HS, Huang SM, Chen KC, Leu YL, Prijovich ZM, Yu CP, Wu CC, Sun GH and Cha TL. Antiangiogenesis targeting tumor microenvironment synergizes glucuronide prodrug antitumor activity. Clin Cancer Res 2009; 15: 4600-4611.

[14] Bosslet K, Straub R, Blumrich M, Czech J, Gerken M, Sperker B, Kroemer HK, Gesson JP, Koch M and Monneret C. Elucidation of the mechanism enabling tumor selective prodrug monotherapy. Cancer Res 1998; 58: 1195-1201.

[15] Tranoy-Opalinski I, Legigan T, Barat R, Clarhaut J, Thomas M, Renoux B and Papot S. beta-Glucuronidase-responsive prodrugs for selective cancer chemotherapy: an update. Eur J Med Chem 2014; 74: 302-313.

[16] Chen X, Wu B and Wang PG. Glucuronides in anti-cancer therapy. Curr Med Chem Anticancer Agents 2003; 3: 139-150.

[17] de Graaf M, Boven E, Scheeren HW, Haisma HJ and Pinedo HM. Beta-glucuronidase-mediated drug release. Curr Pharm Des 2002; 8: 1391-1403.

[18] Wang L, Yang C, Xie C, Jiang J, Gao M, Fu L, Li Y, Bao X, Fu H and Lou L. Pharmacologic characterization of fluzoparib, a novel poly (ADP-ribose) polymerase inhibitor undergoing clinical trials. Cancer Sci 2019; 110: 1064-1075.

[19] Dawicki-McKenna JM, Langelier MF, DeNizio JE, Riccio AA, Cao CD, Karch KR, McCauley M, Steffen JD, Black BE and Pascal JM. PARP-1 activation requires local unfolding of an autoinhibitory domain. Molecular Cell 2015; 60: 755-768.

[20] Wang L, Xu Y, Fu L, Li Y and Lou L. (5R)-5-hydroxytriptolide (LLDT-8), a novel immunosuppressant in clinical trials, exhibits potent antitumor activity via transcription inhibition. Cancer Lett 2012; 324: 75-82.

[21] Salmas RE, Unlu A, Yurtsever M, Noskov SY and Durdagi S. In silico investigation of PARP-1 catalytic domains in holo and apo states for the design of high-affinity PARP-1 inhibitors. J Enzyme Inhib Med Chem 2016; 31: 112-120.

[22] Huang RX and Zhou PK. DNA damage response signaling pathways and targets for radiotherapy sensitization in cancer. Signal Transduct Target Ther 2020; 5: 60.

[23] Sampson VB, Vetter NS, Kamara DF, Collier AB, Gresh RC and Kolb EA. Vorinostat enhances cytotoxicity of SN-38 and temozolomide in ewing sarcoma cells and activates STAT3/AKT/MAPK pathways. PLoS One 2015; 10: e0142704.

[24] Fong PC, Boss DS, Yap TA, Tutt A, Wu P, Mergui-Roelvink M, Mortimer P, Swaisland H, Lau A, O'Connor MJ, Ashworth A, Carmichael J, Kaye SB, Schellens JH and de Bono JS. Inhibition of poly (ADP-ribose) polymerase in tumors from BRCA mutation carriers. N Engl J Med 2009; 361: 123-134.

[25] LaFargue CJ, Dal Molin GZ, Sood AK and Coleman RL. Exploring and comparing adverse events between PARP inhibitors. Lancet Oncol 2019; 20: e15-e28.

[26] Sun K, Mikule K, Wang Z, Poon G, Vaidyanathan A, Smith G, Zhang ZY, Hanke J, Ramaswamy S and Wang J. A comparative pharmacokinetic study of PARP inhibitors demonstrates favorable properties for niraparib efficacy in preclinical tumor models. Oncotarget 2018; 9: 37080-37096.

[27] Drean A, Lord CJ and Ashworth A. PARP inhibitor combination therapy. Crit Rev Oncol Hematol 2016; 108: 73-85.

[28] Wahner Hendrickson AE, Menefee ME, Hartmann LC, Long HJ, Northfelt DW, Reid JM, Boakye-Agyeman F, Kayode O, Flatten KS, Harrell MI, Swisher EM, Poirer GG, Satele D, Allred J, Lensing JL, Chen A, Ji J, Zang Y, Erlichman C, Haluska P and Kaufmann SH. A phase I clinical trial of the poly (ADP-ribose) polymerase inhibitor veliparib and weekly topotecan in patients with solid tumors. Clin Cancer Res 2018; 24: 744-752.

[29] Chabanon RM, Muirhead G, Krastev DB, Adam J, Morel D, Garrido M, Lamb A, Henon C, Dorvault N, Rouanne M, Marlow R, Bajrami I, Cardenosa ML, Konde A, Besse B, Ashworth A, Pettitt SJ, Haider S, Marabelle A, Tutt AN, Soria JC, Lord CJ and Postel-Vinay S. PARP inhibition enhances tumor cell-intrinsic immunity in ERCC1-deficient non-small cell lung cancer. J Clin Invest 2019; 129: 1211-1228.

[30] Friedlander M, Meniawy T, Markman B, Mileshkin L, Harnett P, Millward M, Lundy J, Freimund A, Norris C, Mu S, Wu J, Paton V and Gao B. Pamiparib in combination with tislelizumab in patients with advanced solid tumours: results from the dose-escalation stage of a multicentre, open-label, phase 1a/b trial. Lancet Oncol 2019; 20: 1306-1315.

[31] Zhao Y, Zhang C, Gao L, Yu X, Lai J, Lu D, Bao R, Wang Y, Jia B, Wang F and Liu Z. Chemotherapy-induced macrophage infiltration into tumors enhances nanographene-based photodynamic therapy. Cancer Res 2017; 77: 6021-6032.

[32] Chen BM, Cheng TL, Tzou SC and Roffler SR. Potentiation of antitumor immunity by antibody-directed enzyme prodrug therapy. Int J Cancer 2001; 94: 850-858.